

First – principles studies of CaX (X = In, Tl) intermetallic compounds

M. OZAYMAN, Y. O. CİFTÇİ*, K. COLAKOĞLU, E. DELİGOZ^a

Gazi University, Department Of Physics, Teknikokullar, 06500, Ankara, Turkey

^aAksaray University, Department Of Physics, 68100, Aksaray, Turkey

Ab initio calculations based on the density functional theory within generalized-gradient (GGA) approximation have been performed to carry out the structural, electronic, elastic, and thermodynamic properties of CaX (X=In, Tl). For the total-energy calculations, we have used the projected augmented plane-wave (PAW) implemented in the Vienna Ab initio Simulation Package (VASP). We have investigated two different structures CsCl (B2) and NaTl (B32), and the present structural results are in excellent agreement with the available experimental works. The quasi-harmonic Debye model have been performed to evaluate the thermodynamics properties for CaX (X=In, Tl) compounds. We have, also, predicted the temperature and pressure variation of the volume, bulk modulus, thermal expansion coefficient, heat capacity and Debye temperature in a wide pressure (0 – 13 GPa) for CaIn and (0-11 GPa) for CaTl and temperature ranges (0- 1800 K).

(Received May 2, 2011; accepted May 25, 2011)

Keywords: CaIn, CaTl, Structural properties, Elastic properties, Electronic properties, Thermodynamical properties, ab initio calculations

1. Introduction

Most of the technologically important I-III compounds are crystallized in B32 [1] phase. The physics and chemistry of these intermetallic compounds have attracted lots of interest due to the bound properties [2-4], low metallic conductivity [5], lattice defect [5,6], dissolve in ammonia and amine [7], low paramagnetism and diamagnetism [8,9].

Theoretically, Christensen[10] has studied the structural phase stability of some I-II and III-V metal compounds in B2 and B32 structures based on the first-principles methods. The chemical bonding and bond lengths of the present compounds have also been subject of the various investigations in the past[11-14]. On the experimental side, the lattice structure has been determined by Zintl et al. [15,16] in their early works utilizing the X-ray diffraction method.

CaIn and CaTl crystallizes in the CsCl-type structure (B2), whereas intermetallic NaTl is the prototype of the Zintl phases (B32 structure) [17]. Both structures, B2 and B32, are superstructures of bcc lattice. Compared to most intermetallic phases(B2) the B32 phases have some unusual physical properties: the nearest neighbors are four like and four unlike atoms, whereas for B2 structure, the nearest neighbors are unlike atoms[18].

The phase diagram of Ca-In alloys obtained by Bruzzone et al.[19] using thermal micrographic and X-ray diffraction analyses has been assessed by Okamoto et al[20]. Donski[21] and Baar [22] have investigated the phase diagram by thermal and metallographic analyses. They found crystal structure and lattice parameter in B2 phases.

Although a few experimental works exist on the CaX (X=In, Tl) compounds, to our knowledge, the data are not available dealing with the structural, mechanical,

electronic and thermodynamical properties of CaX (X=In, Tl), and the present work aims to complete these lacks. This work presents the structural, electronic, thermodynamical, and elastic properties in CsCl (B2) and NaTl (B32) phase of CaX (X=In, Tl). In Section 2, a brief outline of the method of calculation is presented. In Section 3, the results are presented followed by a summary discussion.

2. Method of calculation

In the present work, all the calculations have been carried out using the Vienna ab initio simulation package (VASP) [23- 24] based on the density functional theory (DFT). The electron-ion interaction was considered in the form of the projector-augmented-wave (PAW) method [25- 26] with plane wave up to an energy of 500 eV. This cut-off was found to be adequate for the structural, elastic properties as well as for the electronic structure. We do not find any significant changes in the key parameters when the energy cut-off is increased from 500 eV to 550 eV. For the exchange and correlation terms in the electron-electron interaction, Perdew and Zunger-type functional [27- 28] was used within the generalized gradient approximation (GGA) [27]. The 12x12x12 Monkhorst and Pack [29] grid of k-points have been used for integration in the irreducible Brillouin zone. Thus, this mesh ensures a convergence of total energy to less than 10^{-5} eV/atom.

We used the quasi-harmonic Debye model to obtain the thermodynamic properties of CaX (X=In, Tl) [30-31], in which the non-equilibrium Gibbs function $G^*(V; P, T)$ takes the form of

$$G^*(V;P,T) = E(V) + PV + A_{\text{vib}}[\theta(V);T] \quad (1)$$

In Eq.(1), $E(V)$ is the total energy for per unit cell of CaX (X=In, Tl), PV corresponds to the constant hydrostatic pressure condition, $\theta(V)$ the Debye temperature and A_{vib} is the vibration term, which can be written using the Debye model of the phonon density of states as

$$A_{\text{vib}}(\theta, T) = nkT \left[\frac{9\theta}{8T} + 3 \ln \left(1 - e^{-\frac{\theta}{T}} \right) - D \left(\frac{\theta}{T} \right) \right] \quad (2)$$

where n is the number of atoms per formula unit, $D \left(\frac{\theta}{T} \right)$ the Debye integral, and for an isotropic solid, θ is expressed as [32]

$$\theta = \frac{\hbar}{k} [6\pi V^{1/2} n]^{1/3} f(\sigma) \sqrt{\frac{B_s}{M}} \quad (3)$$

where M is the molecular mass per unit cell and B_s the adiabatic bulk modulus, which is approximated given by the static compressibility [33]:

$$B_s \approx B(V) = V \frac{d^2 E(V)}{dV^2} \quad (4)$$

$f(\sigma)$ is given by Refs. [32-34] as

$$f(\sigma) = \left\{ 3 \left[2 \left(\frac{2(1+\sigma)}{3(1-2\sigma)} \right)^{3/2} + \left(\frac{1(1+\sigma)}{3(1-\sigma)} \right)^{3/2} \right]^{-1} \right\}^{1/3} \quad (5)$$

σ is Poisson ratio and the Poisson ratios are used as 0,37 and 0.33 for B32 phases of CaIn and CaTl, respectively. $n=4$ $M=154.896$ a.u for CaIn and, $n=4$ $M=244.4613$ for CaTl. Therefore, the non-equilibrium Gibbs function $G^*(V; P, T)$ as a function of $(V; P, T)$ can be minimized with respect to volume V .

$$\left[\frac{\partial G^*(V; P, T)}{\partial V} \right]_{P, T} = 0 \quad (6)$$

By solving Eq. (6), one can obtain the thermal equation-of-equation (EOS) $V(P, T)$. The heat capacity at constant volume C_v , the heat capacity at constant pressure C_p , and the thermal expansion coefficient α are given [35] as follows:

$$C_v = 3nk \left[4D \left(\frac{\theta}{T} \right) - \frac{3\theta/T}{e^{\theta/T} - 1} \right] \quad (7)$$

$$S = nk \left[4D \left(\frac{\theta}{T} \right) - 3 \ln(1 - e^{-\theta/T}) \right] \quad (8)$$

$$\alpha = \frac{\gamma C_v}{B_T V} \quad (9)$$

$$C_p = C_v (1 + \alpha \gamma T) \quad (10)$$

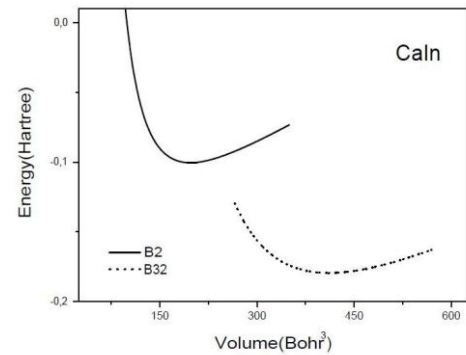
Here γ represent the Grüneisen parameter and it is expressed as

$$\gamma = - \frac{d \ln \theta(V)}{d \ln V} \quad (11)$$

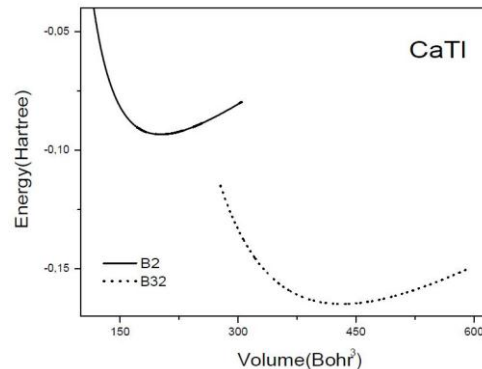
3. Results and discussion

3.1. Structural and electronic properties

Firstly, the equilibrium lattice parameters have been computed by minimizing the crystal total energy calculated for different values of lattice constant by means of Murnaghan's equation of state (eos) [36] as in Fig. 1. (a) and (b). The bulk modulus and its pressure derivative have also been calculated based on the same Murnaghan's equation of state and the results are given in Table 1 along with the experimental and other theoretical values. The calculated value of lattice parameters are 3.8775 \AA in B2 (CsCl) phase, 7.86115 \AA in NaTl (B32) phase for CaIn and 3.9056 \AA in B2(CsCl) phase, 7.9883 \AA in NaTl (B32) phase, respectively. The present values for lattice constants are also listed in Table 1 and the obtained results are quite accord with the other experimental values [19, 37-42].



(a)



(b)

Fig. 1. Total energy versus volume curves for B2 and B32 phases of (a) CaIn and (b) CaTl

Table 1. Calculated equilibrium lattice constant (a_0), bulk modulus (B), pressure derivatives of bulk modulus (B') and other theoretical results for B2 and B32 phases of CaX (X=In, Tl)

Material	Structure	Reference	Lattice parameter (Å)		
			a	B(GPa)	B'
CaIn	B2	Present	3.8775	32.7396	4.0713
		Experimental[21]	3.8191		
		Experimental[3]	3.8560		
	B32	Present	7.8611	27.5430	4.1915
CaTl	B2	Present	3.9056	29.9342	4.2822
		Experimental[22]	3.8550		
		Experimental[23]	3.8470		
		Experimental[24]	3.8522		
		Experimental[25,26]	3.8550		
	B32	Present	7.9883	25.0816	4.3273

We have plotted the phase diagrams (equation of state) for both B2 and B32 phases in Fig. 2. (a) and (b) for CaIn and CaTl, respectively. The discontinuity in volume takes place at the phase transition pressure. The phase transition pressures from B2 to B32 structure is found to be 13.0 GPa and 11.0 GPa from the Gibbs free energy at 0 K for CaIn and CaTl, respectively. The related enthalpy versus pressure graphs for the both phases are shown in Fig. 3. The transition pressure is a pressure at which $H(p)$ curves for both phases crosses.

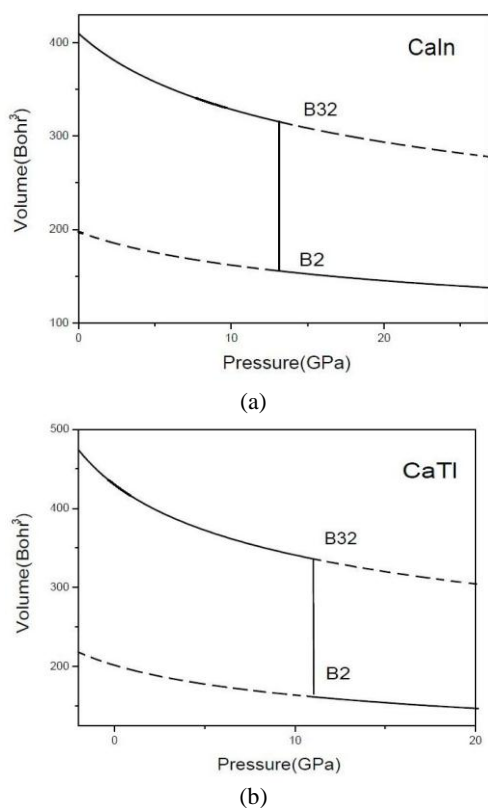


Fig. 2. Pressure versus volume curves of (a) CaIn and (b) CaTl.

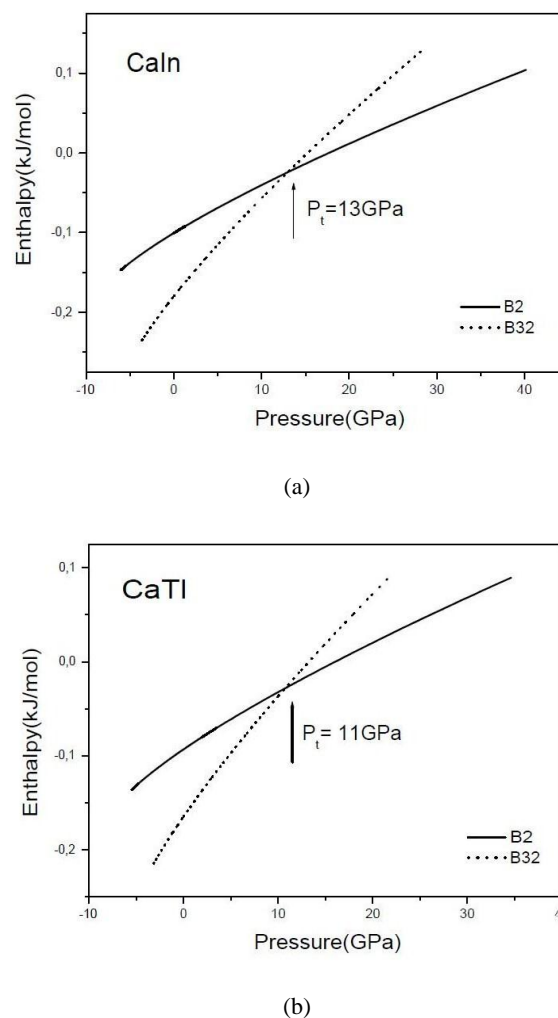


Fig. 3. Estimation of phase transition pressure from B2 to B32 of (a) CaIn and (b) CaTl

The present first – principles code (VASP) have also been used to calculate the band structures for CaIn and

CaTl. The obtained results for high symmetry directions are shown in Fig. 4 (a), (b) for B32 structures of CaIn and CaTl, respectively. It can be seen from the Fig. 4 (a), (b) that no band gap exists for studied compounds, and they exhibit metallic character. The total and partial density of states (DOS and PDOS) corresponding to band structures shown in Fig 4(a) and Fig 4(b) for B32 phases of CaIn and CaTl, respectively, are indicated in Fig 5(a) and Fig. 5(b) along with Fermi energy level. The position of the Fermi level is at 0 eV. In Fig. 5(a), the lowest valance bands occur between about -8.2 and -6.5 eV are essentially dominated by In-s states. Other valance bands are essentially dominated by In-p, Ca-p and Ca-d states. The energy region just above Fermi energy level are dominated by unoccupied Ca-d states. The results indicate that there is a strong hybridization between the In states and Ca states.

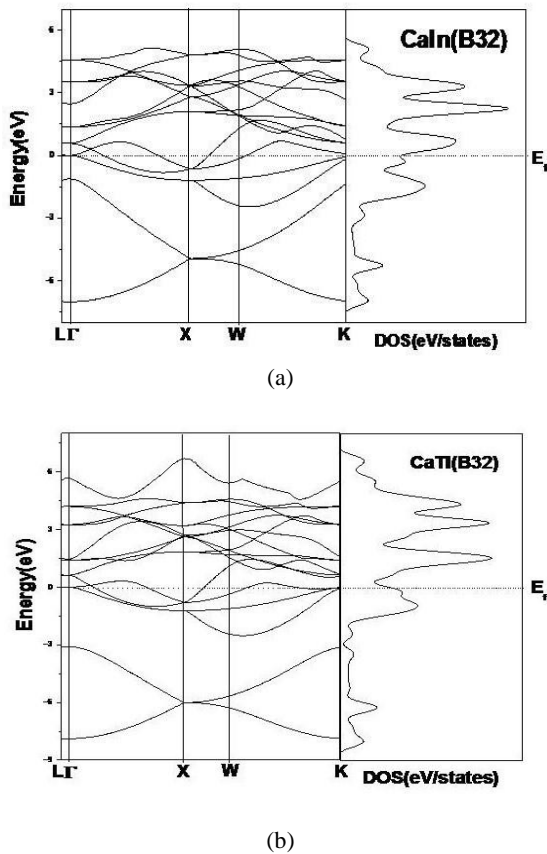


Fig. 4. Calculated band structure of phase B32 of (a) CaIn and (b) CaTl.

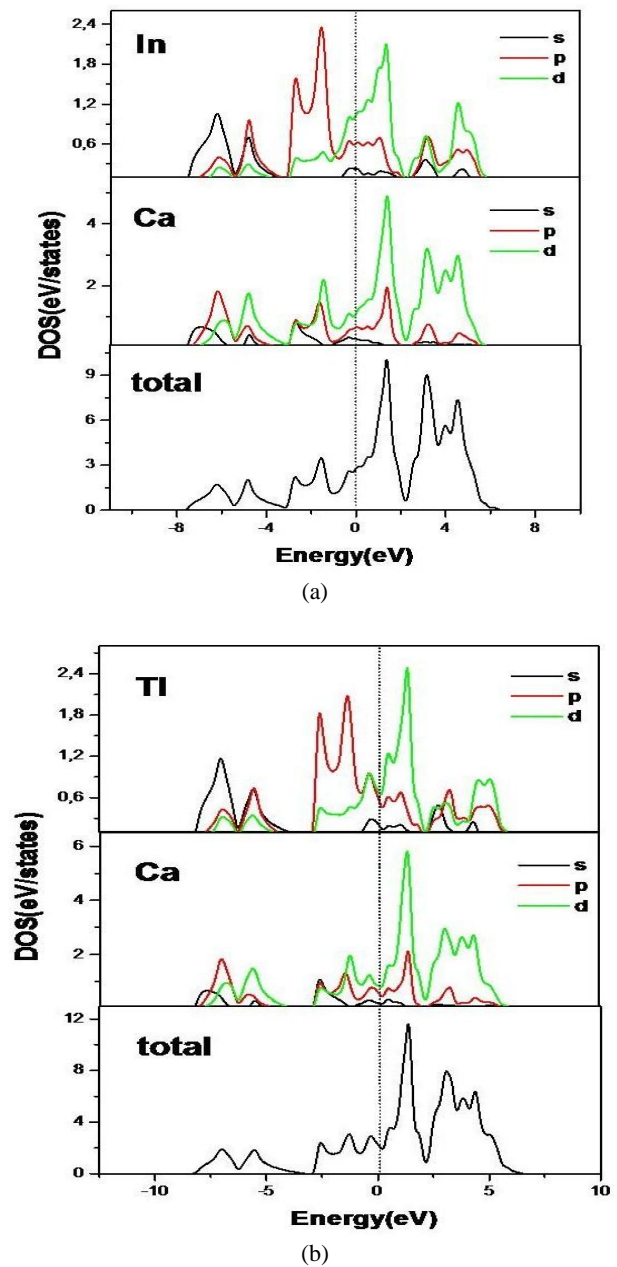


Fig. 5. Partial and total DOS for B32 phase of (a) CaIn (b)CaTl.

3.2 Elastic properties

The elastic constants of solids provide a link between the mechanical and dynamical behaviour of crystals, and give important information concerning the nature of the forces operating in solids. In particular, they provide information on the stability and stiffness of materials. Their ab-initio calculation requires precise methods, since the forces and the elastic constants are functions of the first and second-order derivatives of the potentials. Their calculation will provide a further check on the accuracy of the calculation of forces in solids. The effect of pressure on the elastic constants is essential, especially, for understanding interatomic interactions, mechanical stability, and phase transition mechanisms. It also provides valuable data for developing interatomic potentials

There are two common methods [43-44] for obtaining the elastic data through the ab-initio modelling of materials from their known crystal structures: an approach based on analysis of the total energy of properly strained

states of the material (volume conserving technique) and an approach based on the analysis of changes in calculated stress values resulting from changes in the strain (stress-strain) method. Here we have used the “stress-strain” relations [45] for obtaining the second-order elastic constants (C_{ij}). The known conditions for the mechanical stability of a cubic crystal are: $C_{11} > 0$, $C_{11} - C_{12} > 0$, $C_{44} > 0$, $C_{11} + 2C_{12} > 0$ and $C_{12} < B < C_{11}$. The listed values for C_{ij} in Table 2 are in reasonable order for B32 phases of CaX (X=In, Tl). But, for B2 phases of CaX (X=In, Tl), an unexpected violation is observed on the Cauchy relation $C_{12} - C_{44} = 2P$ (P : Pressure), i. e., our calculations give negative $C_{12} - C_{44}$ values (see Table 2). According to Pettifor [46], the angular character of atomic bonding in metals and compounds can be explained in terms of the negative Cauchy pressure, i.e., the Cauchy pressure may become negative for the directional bonding in some ductile (such as Ni and Al)/brittle (such as Si) materials. The experimental and theoretical values of C_{ij} for CaX (X=In, Tl) are not available at present.

Table 2. The calculated elastic constants (in GPa unit) for B2 and B32 phases of CaX (X=In, Tl).

Material	Structure	C_{11}	C_{12}	C_{44}
CaIn	B2	48.7418	28.0756	33.5367
	B32	36.6533	12.2728	5.3489
CaTl	B2	51.4724	22.0031	26.4096
	B32	32.6521	12.0222	9.0609

For the investigation of their hardness, the elastic properties e.g. the Zener anisotropy factor (A), Poisson's ratio (ν), and Young's modulus (E) are often measured for polycrystalline materials. The Zener anisotropy factor A is calculated using the relation given as [47]:

$$A = \frac{2C_{44}}{C_{11} - C_{12}}, \quad (12)$$

$$\nu = \frac{1}{2} \left[\frac{B - \frac{2}{3}G}{B + \frac{1}{3}G} \right], \quad (13)$$

and

$$Y = \frac{9GB}{G + 3B} \quad (14)$$

where $G = (G_V + G_R)/2$ is the isotropic shear modulus, G_V is Voigt's shear modulus corresponding to the upper bound of G values and G_R is Reuss's shear modulus corresponding to the lower bound of G values and can be written as $G_V = (C_{11} - C_{12} + 3C_{44}) / 5$ and $5/G_R = 4 / (C_{11} - C_{12}) + 3/C_{44}$. The calculated Zener anisotropy factor (A), Poisson ratio (ν), Young's modulus (Y), isotropic shear modulus, G , and B/G for CaX (X=In, Tl) are presented in Table 3.

Table 3. The calculated Zener anisotropy factor (A), Poisson ratio (ν), Young's modulus (Y), isotropic Shear modulus (G) and B/G for CaX (X=In, Tl) for B2 and B32 phases of CaX (X=In, Tl)

Material		A	ν	Y (GPa)	G (GPa)	B/G
CaIn	B2	3.24	0.23	51.82	20.91	1.56
	B32	0.44	0.37	20.61	7.49	3.67
CaTl	B2	1.79	0.22	50.85	20.89	1.43
	B32	0.87	0.33	25.41	9.54	2.63

The Zener anisotropy factor A is a measure of the degree of elastic anisotropy in solids. The A takes the value of 1 for a completely isotropic material. If the value of A smaller or greater than unity it shows the degree of elastic anisotropy. The calculated Zener anisotropy factors for CaX (X=In, Tl) are lower than 1 for B32 phases and greater than 1 for B2 phases which indicates that these compounds are anisotropic materials.

The Poisson's ratio ν and Young's modulus Y are very important properties for industrial applications. The Poisson's ratio ν , provides more information about the characteristics of the bonding forces than any of the other elastic constants. The lower limit and upper limit of Poisson's ratio ν are given 0.25 and 0.5 for central forces in solids, respectively [48]. It is small ($\nu=0.1$) for covalent materials, and it has a typical value of $\nu=0.25$ for ionic materials [49]. Calculated ν values are equal to 0.23 and 0.21 for B2 phases of CaX (X=In, Tl), respectively, 0.37 and 0.33 for B32 phases of CaX (X=In, Tl), respectively, at 0 GPa pressure. It shows that, the ionic contributions to the atomic bonding are dominant for B2 phases of these compounds. In the central force mode, the deviation from the Cauchy relation $\delta=C_{12}-C_{44}$ is a measure of the contribution from the noncentral many-body force since the Cauchy relation should be satisfied when interatomic potentials are purely central. The Young's modulus Y , the ratio between stress and strain, is required to provide information about the measure of the stiffness of the solids. The present values of Young's moduli decrease from B2 phases to B32 phases of CaX (X=In, Tl), which implies that B32 phases of CaX (X=In, Tl) are stiffer than B2 phases of CaX (X=In, Tl).

The bulk modulus is a measure of resistance to volume change by applied pressure, whereas the shear modulus is a measure of resistance to reversible deformations upon shear stress [50]. Therefore, by using the isotropic shear modulus, the hardness of a material can be determined more accurately than by using the bulk modulus. The calculated isotropic shear modulus decreases from B2 phases to B32 phases of CaX (X=In, Tl). We can conclude that the B32 phases of CaX (X=In, Tl) are softer than B2 phases of CaX (X=In, Tl) which accords with the results as previously noted in the paragraph related to Young's modulus Y .

We can also estimate the brittle/ductile behaviour of this compound using the calculated bulk modulus and isotropic shear modulus. According to the criterion, proposed by Pugh [51], a material is brittle if the B/G ratio is less than 1.75, otherwise it behaves in ductile manner. The present value of B/G is found to be 1.56 and 1.43 for B2 phases of CaX (X=In, Tl), respectively, and 3.67 and 2.63 for B32 phases of CaX (X=In, Tl), respectively. In our B2 phase case, these parameters are less than 1.75, i.e. B2 phase of these materials will behave in a brittle manner. In our B32 phase case, B/G are greater than 1.75, which means that B32 phases of CaX (X=In, Tl) will behave in ductile.

3.3 Thermodynamics Properties

The thermal properties are determined in the temperature range from 0 to 1800 K for CaX (X=In, Tl), where the quasi-harmonic model remains fully valid. The pressure effect is studied in the 0-13.0 GPa and 0-11.0 GPa range for CaIn and CaTl, respectively. The relationship between normalized volume and pressure at different temperature is shown in Fig. 6 (a), (b) for CaX (X=In, Tl). It can be seen that when the pressure increases from 0 GPa to 13.0 GPa, 11.0 GPa the volume decreases, respectively. The reason of this changing can be attributed to the atoms in the interlayer become closer, and their interactions become stronger. For CaX (X=In, Tl) compound the normalized volume decreases with increasing temperature.

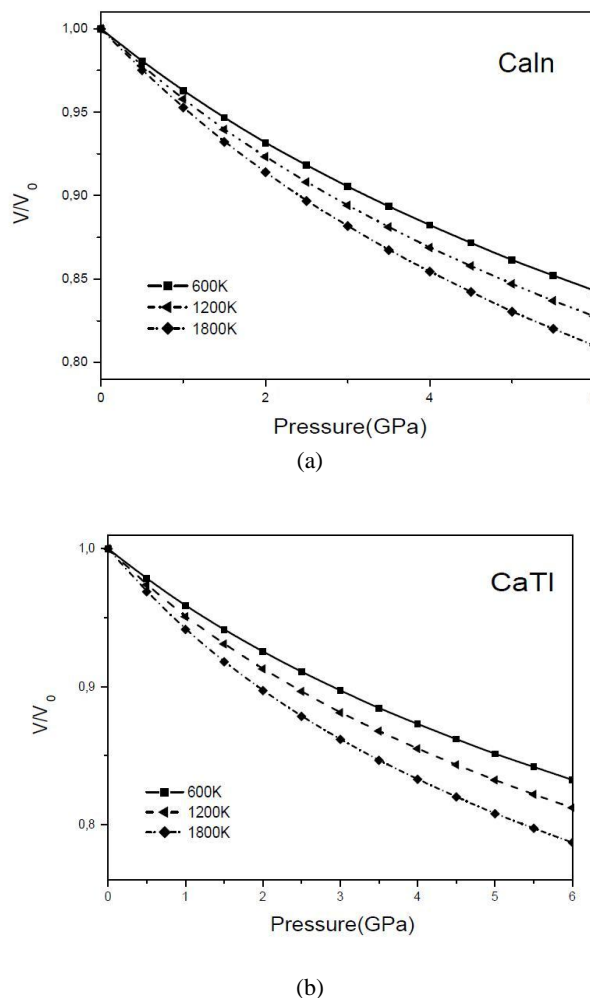


Fig. 6. The normalized volume-pressure diagram of the B2 and B32 phases of (a) CaIn and (b) CaTl at different temperatures.

The variations of the thermal expansion coefficient (α) with temperature and pressure are shown in Figure 7 (a), (b) and Fig. 8 (a), (b) for CaX (X=In, Tl), respectively. It is shown that, the thermal expansion coefficient α also increases with T at lower temperatures and gradually approaches linear increases at higher temperatures, while the thermal expansion coefficient α decreases with pressure. At different temperature, α decreases nonlinearly at lower pressure and decreases almost linearly at higher pressure. Also, It can be seen from Fig. 8 (a) that the temperature dependence of α is very small at high temperature and higher pressure.

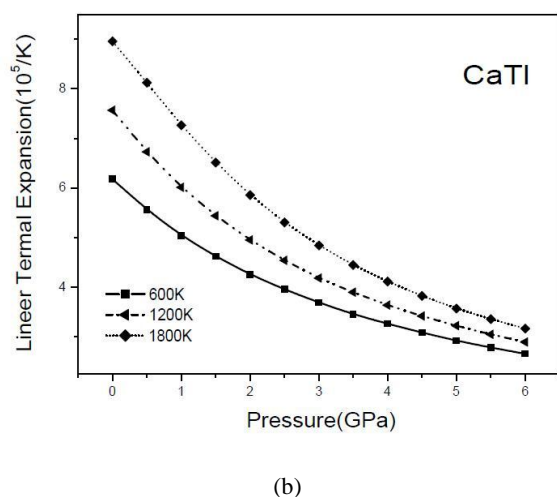
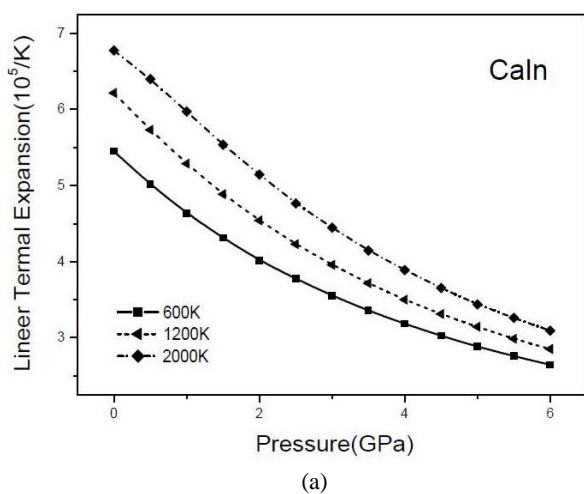


Fig. 7. The thermal expansion versus pressure for B32 phase of (a) CaIn (b) CaTl.

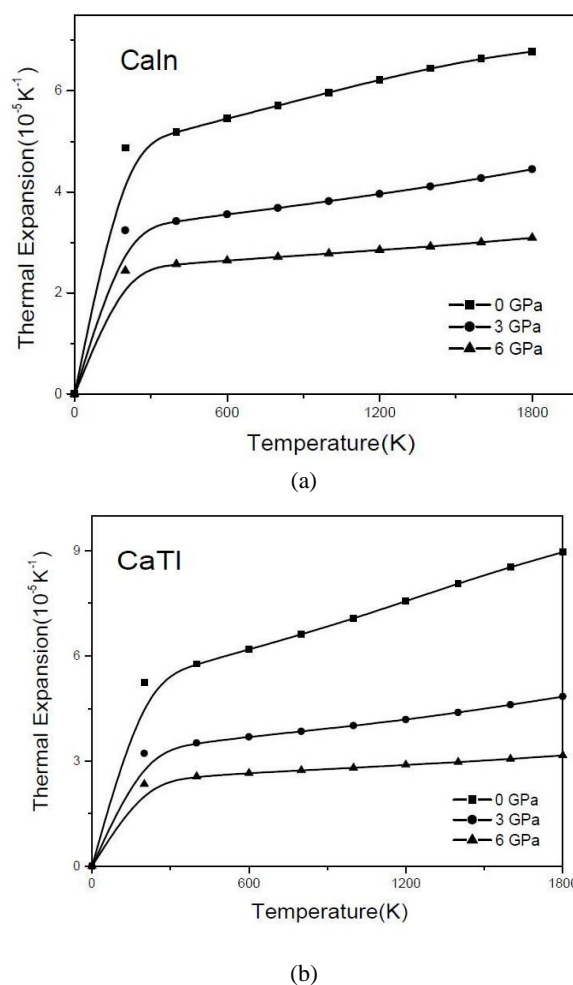


Fig. 8. The thermal expansion versus temperature for B32 phase (a) CaIn (b) CaTl.

Temperature effects on bulk modulus (B) are given in Fig. 9 (a), (b) and can be seen that B decreases as temperature increases. Because cell volume changes rapidly as temperature increases. The relationship between bulk modulus (B) and pressure (P) at different temperatures (600, 1200, and 1800K) are shown in Fig. 10 (a), (b) for CaX (X=In, Tl). It can be seen that bulk modulus decreases with the temperature at a given pressure and increases with pressure at a given temperature. It shows that the effect of increasing pressure on Ca (X=In, Tl) is the same as decreasing the temperature.

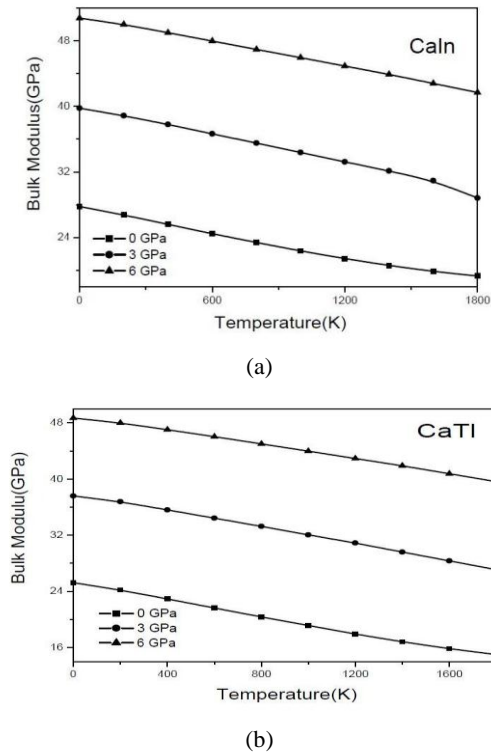


Fig. 9. The bulk modulus (B) as a function temperature (T) at $P=0$ for B32 phase (a) CaIn and (b) CaTl.

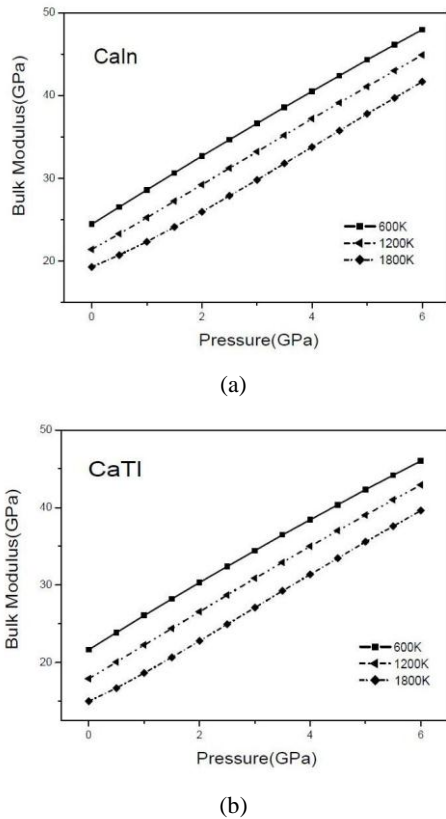


Fig. 10. The relation between bulk modulus (B) and pressure P (a) at temperatures of 600K, 1200K, 1800K of B32 phase of CaIn (b) at temperatures of 400 K, 1200 K, 2000 K of B32 phases of CaTl.

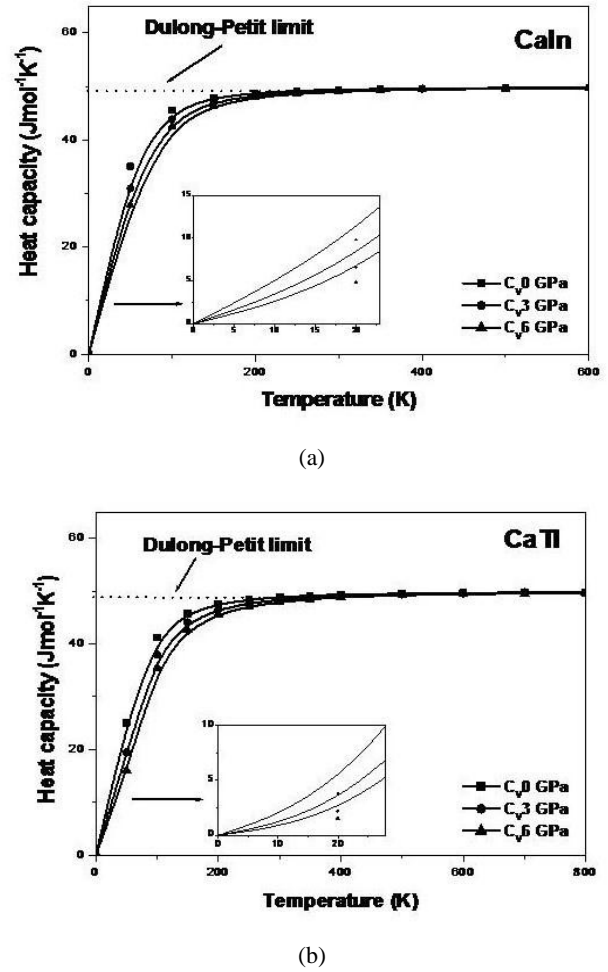


Fig. 11. The variation of C_v with temperature at different pressures for B32 phase of (a) CaIn (b) CaTl.

For the temperature-dependent behavior of bulk modulus, the third-order polynomial fitting gives the following equations for B32 phase at 0GPa:

$$B = 27.78989 - 5.33 \times 10^{-3} T - 6.53555 \times 10^{-7} T^2 + 5.50699 \times 10^{-10} T^3$$

for CaIn

$$B = 25.26256 - 5.29 \times 10^{-3} T - 1.6167 \times 10^{-6} T^2 + 7.75544 \times 10^{-10} T^3$$

for CaTl

The value of bulk modulus (27.78 GPa for CaIn and 25.26 GPa for CaTl) from the fitting procedure at $P=0$ GPa and $T=0$ K is close to our previous result in Table 1.

The calculated properties at different temperatures are very sensitive to the vibrational modes. In the quasi-harmonic Debye model, the Grüneisen parameter, $\gamma(T)$, and the Debye temperature, $\theta(T)$, are two key quantities. These quantities at various temperatures (0 -1800 K) and different pressures (0, 3, 6 GPa) are calculated and the

results are shown in Table 4 and 5 for CaX (X=In, Tl) compounds. It is clear from Table 5 and 6 that as

temperature increases, the Grüneisen parameter decreases and the Debye temperature increases.

Table 4. The calculated Debye temperature θ (K) over a wide range of temperatures and pressures for B32 phase of CaX (In and Tl) compounds.

T (K)	CaIn			CaTl		
	P (GPa)			P (GPa)		
	0	3	6	0	3	6
0K	138.22	163.07	182.25	200.39	240.95	271.2
200K	136.14	161.7	181.2	197.4	239.32	269.88
400K	133.43	159.88	179.72	192.88	236.3	297.68
600K	130.6	157.85	178.21	188.08	233.17	265.41
800K	127.72	155.8	176.66	182.92	229.96	263.07
1000K	124.65	153.69	175.08	177.71	226.63	260.67
1200K	121.54	151.52	173.46	171.8	223.37	258.2
1400K	118.4	149.37	171.92	165.82	219.6	255.85
1600K	115.14	146.97	170.15	159.63	215.76	253.15

Table 5 The calculated Grüneisen parameter over a wide range of temperatures and pressures for B32 phase of CaX (In and Tl) compounds.

T (K)	CaIn			CaTl		
	P (GPa)			P (GPa)		
	0	3	6	0	3	6
0K	1.957	1.744	1.592	2.052	1.778	1.603
200K	1.975	1.755	1.6	2.073	1.788	1.61
400K	1.997	1.77	1.611	2.106	1.807	1.622
600K	2.02	1.787	1.622	2.14	1.827	1.634
800K	2.042	1.805	1.634	2.160	1.848	1.647
1000K	2.065	1.823	1.646	2.212	1.87	1.661
1200K	2.085	1.842	1.659	2.251	1.892	1.675
1400K	2.103	1.861	1.671	2.287	1.917	1.688
1600K	2.118	1.881	1.686	2.319	1.944	1.704

The temperature –dependent behavior of the constant-volume heat capacity, C_v , at various pressures P are shown in Fig. 11 a and b for CaX (X=In, Tl) compounds, respectively. It is seen from these figures that when $T < 300$ K, C_v increases very rapidly with temperature; when $T > 400$ K, C_v increases slowly with temperature and it almost approaches a constant called as Dulong-Petit limit ($C_v(T) \sim 3R$ for mono atomic solids) at higher temperatures for CaX (X=In, Tl) compounds.

4. Summary and conclusions

In summary, the first principles calculations have been performed to obtain structural, elastic, electronic and thermodynamic properties of CaX (X=In, Tl) compounds. The structural parameters (the lattice parameters and bulk modulus) are in good agreement with the previous

experimental data. Our results for elastic constants satisfy the traditional mechanical stability conditions for B32 phases of CaX (X=In, Tl) compounds. Other mechanical data such as Zener anisotropy factor (A), Poisson's ratio (ν), Young's modulus (E), and isotropic shear modulus (G) are determined for the first time. Some basic thermodynamical quantities such as the heat capacity (C_v), thermal expansion (α) coefficient, Grüneisen parameter (γ), and the Debye temperature (θ_D) are calculated based on the quasi-harmonic Debye model at various temperatures and pressures, and the results are interpreted.

Acknowledgments

This work is supported by Gazi University Research – Project unit under Project No: 05/2010-51.

References

- [1] E. Zintl, G. Brauer, *Z. Phys. Chem. B* **20**, 245 (1933).
- [2] H. Schafer, B. Eisenmann, W. Muller, *Angew. Chem. Int. Ed. Engl.* **12**, 694 (1973).
- [3] P.C. Schmidt, *Z. Naturforsch A* **40**, 335 (1985).
- [4] S. Kauzlarich (Ed.) *Chemistry, Structure and Bonding of Zintl Phases and Ions*, VCH Publishers, New York, 1996.
- [5] K. Kishio, J. O. Brittain, *J. Phys. Chem. Solids* **40**, 933 (1979).
- [6] R. Wilhite, N. Karnezos, P. Cristea, J.O. Brittain, *J. Phys. Chem. Solids* **37**, 1073 (1976).
- [7] A. J. Downs, *Chemistry of Aluminium, Gallium, Indium and Thallium*, Chapman & Hall, London, 1993.
- [8] Y. L. Yao, *Trans. Metall. Soc. AIME* **230**, 1725 (1964).
- [9] V. W. Klemm, H. Fricke, *Zeitschrift Fur Anorganische Und Allgemeine Chemie* **282**, 162 (1955).
- [10] N. E. Christensen, *Phys. Rev. B* **32**(1), 207 (1985).
- [11] M.B. McNeil, W.B. Pearson, L.H. Bennett, R.E. Watson, *J. Phys. C: Solid State Phys.* **6**, 1 (1973).
- [12] A.M. Aslan, *Int. J. Chem.* **10**(1), 17 (2000).
- [13] J.E. Inglesfield, *J. Phys. C: Solid State Phys.* **4**, 1003 (1971).
- [14] Z. Pawloska, N.E. Christensen, S. Satpathy, O. Jepsen, *Phys. Rev. B* **34**(10), 7080 (1986).
- [15] E. Zintl, S. Neumayr, *Z. Phys. Chem. B* **20**, 272 (1933).
- [16] E. Zintl, W. Dullenkopf, *Z. Phys. Chem. B* **16**, 195 (1932).
- [17] E. Zintl, P. Woltersdorf, *Z. Elektrochem.* **41**, 876 (1935).
- [18] P.C. Schmidt, *Phys. Rev. B*, **31**(8), 5015 (1985).
- [19] G. Bruzzone, A.F. Ruggiero, *J. Less-Common Met.* **7**, 368 (1964).
- [20] H. Okamoto, V.P. Itkin, C.B. Alcock, *J. Phase Equilibria*, **12**, 379 (1991).
- [21] L. Donksi, *Z. Anorg. Chem.* **57**, 206 (1908).
- [22] N. Baar, *Z. Anorg. Chem.* **70**, 366 (1911).
- [23] G. Kresse, J. Hafner, *Phys. Rev. B*, **47**, 558 (1994).
- [24] G. Kresse and J. Furthmüller, *Phys. Rev. B*, **54**, 11169 (1996).
- [25] G. Kresse, D. Joubert, *Phys. Rev. B* **59**, 1758 (1999).
- [26] P. E. Blochl, *Phys. Rev. B*, **50**, 17953 (1994).
- [27] J. P. Perdew, A. Zunger, *Phys. Rev. B*, **23**, 5048 (1981).
- [28] J. P. Perdew, J. A. Chevary, S. H. Vosko, K. A. Jackson, M. R. Pederson, D. J. Singh, C. Fiolhais, *Phys. Rev. B* **46**, 6671 (1992).
- [29] H. J. Monkhorst, J. D. Pack, *Phys. Rev. B*, **13**, 5188 (1976).
- [30] M.A. Blanco, E. Francisco, V. Lunana, *Comput. Phys. Commun.*, **158**, 57 (2004).
- [31] F. Peng, H.Z. Fu, X.D. Yang, *Physica B*, **403**, 2851 (2008).
- [32] M.A. Blanco, A.M. Pendàs, E. Francisco, J.M. Recio, R. Franko, *J. Mol. Struct. (Theochem)* **368**, 245 (1996).
- [33] M. Flórez, J. M. Recio, E. Francisco, M.A. Blanco, A.M. Pendàs, *Phys. Rev. B* **66**, 144112 (2002).
- [34] E. Francisco, J.M. Recio, M. A. Blanco, A. M. Pendàs, *J. Phys. Chem.* **102**, 1595 (1998).
- [35] R. Hill, *Proc. Phys. Soc. Lond. A* **65**, 349 (1952).
- [36] F. D. Murnaghan, *Proc. Natl., Acad. Sci. USA* **30**, 5390 (1994).
- [37] J. D. Marcoll., P.C. Schmidt., A. Weiss, *Z. Naturforsch. A* **29**, 473 (1974).
- [38] G. Bruzzone, *Ann. Chim. (Rome)* **56**, 1306 (1966).
- [39] E. Zintl, C. Brauer, *Z. Phys. Chem., Abt. B* **20**, 245 (1933).
- [40] J.D. Marcoll., P.C. Schmidt, A. Weiss, *Z. Naturforsch. A* **29**, 473 (1974).
- [41] E. Zintl, S. Neumayr, *Z. Elektrochem.* **39**, 86 (1933).
- [42] G. Bruzzone, *Ann. Chim. (Rome)* **56**, 1306 (1966).
- [43] J. Mehl, *Phys. Rev. B* **47**, 2493 (1993).
- [44] S.Q. Wang, H.Q. Ye, *Phys. Status Solidi B* **240**, 45 (2003).
- [45] O. H. Nielson, R.M. Martin, *Phys. Rev. Lett.* **50**, 697 (1983).
- [46] D. G. Pettifor, *Mater. Sci. Technol.* **8**, 345 (1992).
- [47] B. Mayer, H. Anton, E. Bott, M. Methfessel, J. Sticht, P. C. Schmidt, *Intermetallics* **11**, 23 (2003).
- [48] H. Fu, D. Li, F. Peng, T. Gao, X. Cheng, *Comput. Mater. Sci.* **44**, 774 (2008).
- [49] V. V. Bannikov, I. R. Shein, A. L. Ivanovskii, *Phys. Status Solidi (RRL)* **1**, 89 (2007).
- [50] A. F. Young, C. Sanloup, E. Gregoryanz, S. Scandolo, R. E. Hemley, H. K. Mao, *Phys. Rev. Lett.* **96**, 155501 (2006).
- [51] S. F. Pugh, *Philos. Mag.* **45**, 823 (1954).

*Corresponding author: yasemin@gazi.edu.tr